



QUASICRYSTALLINE PHASES AND THEIR APPROXIMANTS IN Al–Mn–Zn ALLOYS

A. SINGH[†], S. RANGANATHAN¹ and L. A. BENDERSKY²

¹Centre for Advanced Study, Department of Metallurgy, Indian Institute of Science, Bangalore-560 012, India and ²National Institute of Standards and Technology, Gaithersburg, MD 20899, U.S.A.

(Received 24 June 1996; accepted 24 January 1997)

Abstract—Two Al–Mn–Zn alloys in melt-spun condition have been studied by transmission electron microscopy. The Al₂₄Mn₅Zn alloy was found to be fully icosahedral, while the Al₁₂Mn_{2.5}Zn alloy gave rise to decagonal quasicrystal. The decagonal phase grew in clusters with an orientation relationship between the grains suggesting nucleation on an icosahedral seed. On annealing at 500–600°C, the quasicrystalline phases transformed to a body centered orthorhombic phase L ($a = 1.24$, $b = 1.26$ and $c = 3.05$ nm) with a high density of planar defects. This phase transforms to an ordered and defect free monoclinic phase M, a superlattice structure of L ($a = c = 1.77$, $b = 3.05$ nm and $\beta = 89.1^\circ$). The L phase is shown to be a rational approximant of the icosahedral phase. The interrelationship among quasicrystalline phases and their rational approximants in Al–Mn–Zn system are highlighted. © 1997 Acta Metallurgica Inc.

1. INTRODUCTION

The discovery of the icosahedral quasicrystal [1] was closely followed by the discovery of a two-dimensional quasicrystal [2, 3], christened decagonal quasicrystal due to the presence of a unique ten-fold axis. Soon, a close relationship between the structure of quasicrystals and some crystalline phases, called rational approximant structures, was established. The structures of these approximants can be generated by substituting the irrational number of τ (the golden mean) with a rational number q/p , where p and q are consecutive numbers in the Fibonacci Series [4, 5]. While several aluminium–transition metal binary and ternary alloys have been studied from the viewpoint of formation of quasicrystals and approximants, the Al–Mn–Zn system has received very little attention.

Raynor and Wakeman [6] have reported the occurrence of three ternary phases in the Al–Mn–Zn system. These phases are designated T1, T2 and T3. T1 phase is given by the formula Al₂₄Mn₅Zn. Robinson [7] has determined the structure of T1 phase to be a C-centered orthorhombic phase with lattice parameters $a = 2.48$, $b = 2.51$ and $c = 3.03$ nm. It is further pointed out by Robinson that the diffraction spots with l odd are weak so that the cell can be mistaken for a body centered one with half the a and c parameters. From Raynor and Wakeman's work [6] the formula for T3 phase can be given by Al₁₁(MnZn)₅. Damjanovic [8] has deduced the structure of T3 phase to be C-centered orthorhombic unit cell with lattice parameters $a = 0.778$, $b = 2.88$ and $c = 1.26$ nm.

The T1 phase has a composition similar to the Al₆₀Mn₁₁Ni₄ [9] and Al₂₀Mn₃Cu₂ [7] phases which have a ratio of four aluminium atoms to one transition metal atom. Robinson [9] showed that the T1 phase is similar in electronic structure to the Al₆₀Mn₁₁Ni₄ and Al₂₀Mn₃Cu₂ phases. However the unit cell dimensions and the structure of these Al–Mn–Ni and Al–Mn–Cu phases are similar to those of the T3 phase [8].

Robinson [9] noted that the structure of the Al₆₀Mn₁₁Ni₄ phase had centered pentagons and there was a pronounced layering of the structure. Ranganathan and Chattopadhyay [10] pointed out the similarity between the decagonal phase and the isostructural ternary phases Al₂₀Mn₃Cu₂, Al₆₀Mn₁₁Ni₄ and T3–AlMnZn. The Al₂₀Mn₃Cu₂ is known to be an approximant to the decagonal quasicrystal and is called Robinson approximant [11]. The decagonal quasicrystal has been obtained by rapid solidification of Al₆₀Mn₁₁Ni₄ and the Al₂₀Mn₃Cu₂ alloys [12–18]. The approximant structures to the decagonal phase have been studied extensively in Al–Mn–Ni [12, 13] and Al–Mn–Cu [14, 15].

Schaefer and Bendersky [19] showed that an addition of zinc to Al–Mn alloys promoted the formation of the decagonal phase. Lilienfeld *et al.* [20] obtained quasicrystals in the alloys with compositions near the isostructural Al₆₀Mn₁₁Ni₄, Al₂₀Mn₃Cu₂ and Al₁₁Mn₃Zn₂ phases by ion beam mixing.

The icosahedral quasicrystal is known to have cubic, rhombohedral and orthorhombic approximants. α -AlMnSi [21] and Mg₃₂(Al, Zn)₄₉ [22] are well known cubic approximants to the icosahedral phase. Examples of the rhombohedral approximants are

[†]To whom all correspondence should be addressed.

found in the Al-Cu-Fe and Al-Cu-Li alloys which are well studied systems. Some work has been done on the orthorhombic icosahedral approximants [23, 24].

The decagonal quasicrystal has two well known orthorhombic approximants called the Robinson, or the R approximant mentioned above and the Taylor, or the T approximant. The T approximant is based on the structure of Al_3Mn first reported by Taylor [25]. These two decagonal approximants have been found to exist in a number of systems such as Al-Mn [26-28] and Al-Mn-Cu [14, 15].

Although quasicrystals and their approximant structures have been extensively studied in Al-Mn-Ni and Al-Mn-Cu systems, very little work has been carried out on the Al-Mn-Zn alloys. We report here a detailed work on the formation of quasicrystals and the approximant structures to the quasicrystals. Two alloys are studied here. One corresponds to the T1 phase with composition given by $Al_{24}Mn_5Zn$ and the other has a composition corresponding to $Al_{12}Mn_{2.9}Zn$, close to T3 phase. A preliminary report of this work has been presented earlier [13].

2. EXPERIMENTAL PROCEDURE

Two alloys of composition $Al_{24}Mn_5Zn$ and $Al_{12}Mn_{2.9}Zn$ were prepared by melting pure metals in an inert atmosphere and rapidly solidified by melt spinning on a copper wheel. The heat treatments were carried out in tubular furnaces after sealing the samples in evacuated and argon backfilled quartz tubes. The samples were characterized by transmission electron microscopy (TEM) on a JEOL 2000FX-II microscope operated at 200 kV after thinning the samples in an ion mill.

3. RESULTS

The melt spun ribbons were 3-4 mm wide. While the ribbons of $Al_{24}Mn_5Zn$ were less brittle and were 30-40 mm long, those of $Al_{12}Mn_{2.9}Zn$ were highly brittle and had a flaky appearance of 3-4 mm length.

3.1. Quasicrystalline phases

The $Al_{24}Mn_5Zn$ ribbons consist entirely of the icosahedral quasicrystal. A microstructure and some electron diffraction patterns from this phase are

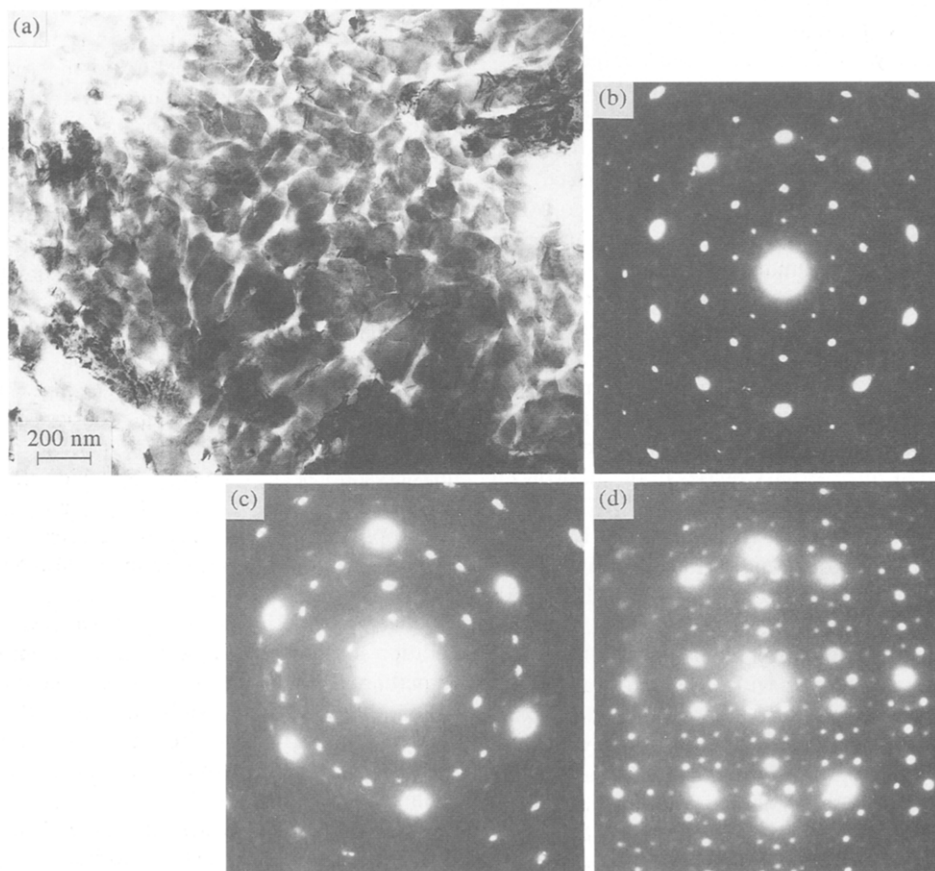


Fig. 1. (a) A bright field electron micrograph showing the microstructure of the icosahedral phase in melt spun $Al_{24}Mn_5Zn$ alloy. (b), (c) and (d) Electron diffraction patterns from the five-, three- and two-fold zone axes of the icosahedral phase, respectively.

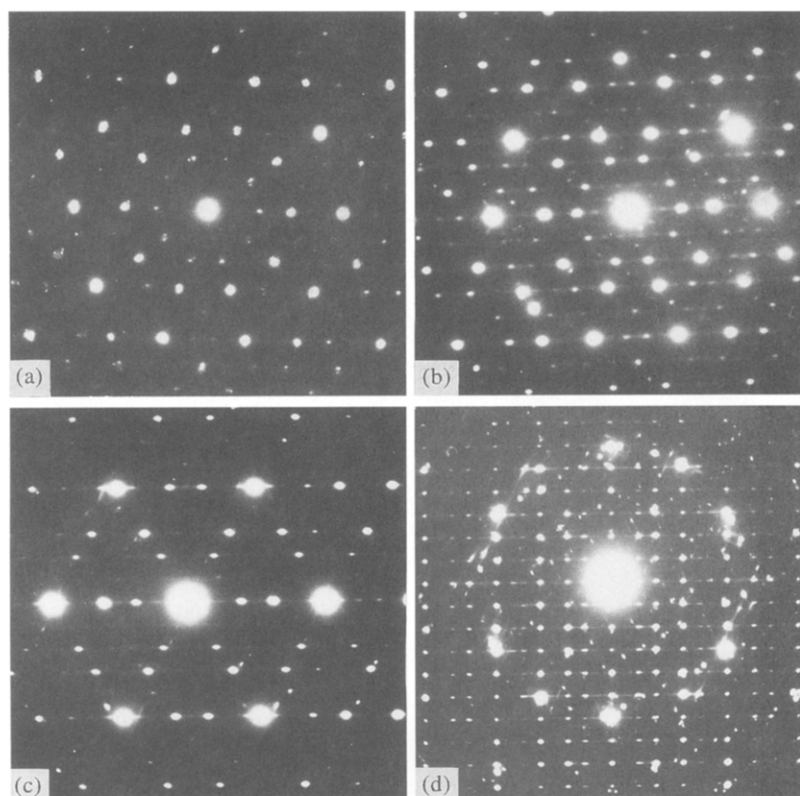


Fig. 2. Electron diffraction patterns from the decagonal phase in the melt spun $\text{Al}_{12}\text{Mn}_{29}\text{Zn}$ alloy (a) ten-fold, (b) pseudo five-fold, (c) pseudo three-fold and (d) the two-fold "G" zone axis.

shown in Fig. 1. The grains have a dendritic morphology, show a speckled contrast, and have an average size of half a micron, as observed in Fig. 1(a).

The $\text{Al}_{12}\text{Mn}_{29}\text{Zn}$ ribbons showed the presence of the decagonal quasicrystal with a periodicity of six, i.e. of about 1.2 nm along the decagonal axis. The electron diffraction patterns shown in Fig. 2 are along (a) the ten-fold, (b) a pseudo five-fold, (c) a pseudo three-fold and (d) a two-fold axis. All the patterns except the ten-fold show streaks due to sheets of diffuse intensity perpendicular to the decagonal axis, a characteristic of the decagonal phase [3, 29].

The typical size of the decagonal grains was found to be of the order of $0.2 \mu\text{m}$. The grains showed striated contrast characteristic of the decagonal phase. The decagonal grains occurred in clusters of a micron size with mutual orientation relationships suggesting that they have grown on a nucleus of an icosahedral phase, although no icosahedral phase was detected. Figure 3(a) shows two grains oriented with a two-fold zone axis, perpendicular to the decagonal axis, along the electron beam. Two variants of this zone axis were observed in the grain, with the decagonal axes separated by 63.4° , equal to the angle between two five-fold axes of an icosahedron. Figure 3(b) shows the domains of these two variants by different orientation of lattice fringes. The directions of the decagonal axis is marked. Figure 3(c) shows the composite diffraction pattern from the two variants.

The prominent zone axes of the decagonal phase are labelled A to Q by Daulton *et al.* [27] and Ranganathan *et al.* [30]. The ten-fold zone axis is labelled A, the two two-fold axes as G and H, and the pseudo five-fold axis as J. There are two pseudo three-fold axes which are labelled I and M. Figures 4(a), (b) show diffraction patterns from the aggregate of the decagonal phase in pseudo three-fold zone axis I orientation. Although the orientation of a hexagon formed by six intense spots is the same in all these diffraction patterns, three variants of this zone axis were observed which are easily distinguished by the direction of the streaks in them. When oriented along the ten-fold axis, the neighbouring grains in the aggregate have orientation of pseudo five-fold (J) zone axis. Five variants of the J axis are observed. Two of these five variants of this zone axis observed along a ten-fold orientation of the aggregate are shown in Fig. 4(c), (d). The orientation of the strong spots is the same but the streaks are oriented differently in these two diffraction patterns.

3.2. Crystalline approximant phases

The melt-spun samples were isothermally aged to study the transformation behaviour of the quasicrystalline phases. On ageing the melt spun $\text{Al}_{12}\text{Mn}_{29}\text{Zn}$ alloy at 500°C for half an hour, the icosahedral quasicrystal transformed to a crystalline phase.

Figure 5 (a)–(c) shows some low index diffraction patterns obtained from this phase. The diffraction pattern in Fig. 5(c) shows streaking and some other patterns showed weak diffraction spots. Ignoring the streaks and weak spots, the diffraction patterns can be indexed to a body centered orthorhombic cell with lattice parameters $a = 1.24$, $b = 1.26$ and $c = 3.05$ nm. Thus the diffraction patterns in Fig. 5

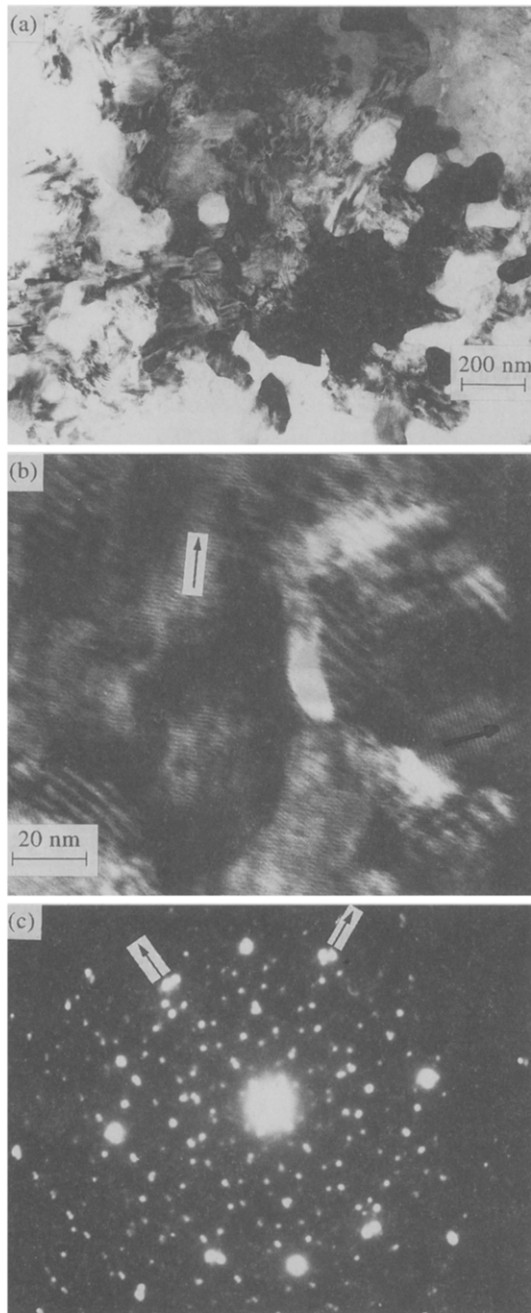


Fig. 3. (a) An aggregate of decagonal grains observed along a two-fold G orientation in melt spun $\text{Al}_{12}\text{Mn}_{29}\text{Zn}$. (b) A high resolution electron micrograph from this cluster shows domains in two orientations of the two-fold G . The periodic direction in both the orientations is marked by arrows. (c) A composite diffraction pattern of the two orientations of G .

can be indexed as (a) [100], (b) [010] and (c) [110] zone axis patterns of this phase. The schematics of [100], [010] and [110] zone axes are shown in Fig. 5(d)–(f). This phase will be referred to as the L phase after Little [31] who first reported a similar phase in Al–Cr, discussed in the next section.

The $\text{Al}_{12}\text{Mn}_{29}\text{Zn}$ alloy containing the decagonal phase transformed fully to a crystalline phase when annealed at 600°C for an hour. This phase is the same as the L phase with similar characteristics that were observed in the diffraction patterns of the L phase obtained on annealing the $\text{Al}_{24}\text{Mn}_5\text{Zn}$ alloy.

The grain sizes of the L phase were typically a micron and the high resolution electron micrographs in both the alloys showed coexistence of another phase with the L phase, associated with a high density of planar defects. This explained the streaking which occurs between the rows of spots parallel to the $[001]^*$ row of spots in the [110] zone axis pattern. This other phase, called M, coexists with L and is its superstructure. A unit cell for the M phase is chosen such that

$$a_M = d_{(1\bar{1}0)_L}, b_M = c_L, c_M = d_{(110)_L}$$

(d denotes interplanar distance).

The lattice parameters of M are deduced to be monoclinic $a = c = 1.77$ nm, $b = 3.05$ nm and $\beta = 89.1^\circ$. This cell is nearly orthorhombic. The orientation relationship between the two phases is,

$$\begin{aligned} [100]_M &\parallel [\bar{1}10]_L \\ [010]_M &\parallel [001]_L \\ [001]_M &\parallel [110]_L \end{aligned}$$

Phases with lattice parameters similar to those of L and M have been reported by Bendersky *et al.* [32] in Al–Cr system.

Figure 6(a) and (b) show the micrographs corresponding to the [010] zone axis of the L phase in the $\text{Al}_{24}\text{Mn}_5\text{Zn}$ alloy aged at 600°C for 4 h. The low magnification micrograph of the grain (Fig. 6(a)) shows a uniform distribution of dark domains. In the accompanying high resolution micrograph (Fig. 6(b)) a unit cell of 1.16×1.16 nm can be defined. A change in the appearance of the lattice fringes in some regions gives it a darker appearance. These regions are those of the phase M. An annealing up to four hours increases the volume fraction of the M phase and its diffraction spots become more defined in place of streaks.

On further annealing of the $\text{Al}_{24}\text{Mn}_5\text{Zn}$ alloy for 25.5 h at 600°C , a hexagonal phase with lattice parameters of $a = 2.84$ and $c = 1.26$ nm appeared, reported as $\lambda\text{Al}_4\text{Mn}$ phase in the literature [33]. Figure 7 shows the [001] and [100] zone axis patterns of this phase. The [001] pattern shows a striking resemblance to the three-fold electron diffraction pattern of an icosahedral phase. Bendersky [34] has reported this phase with the [001] diffraction pattern from this phase.

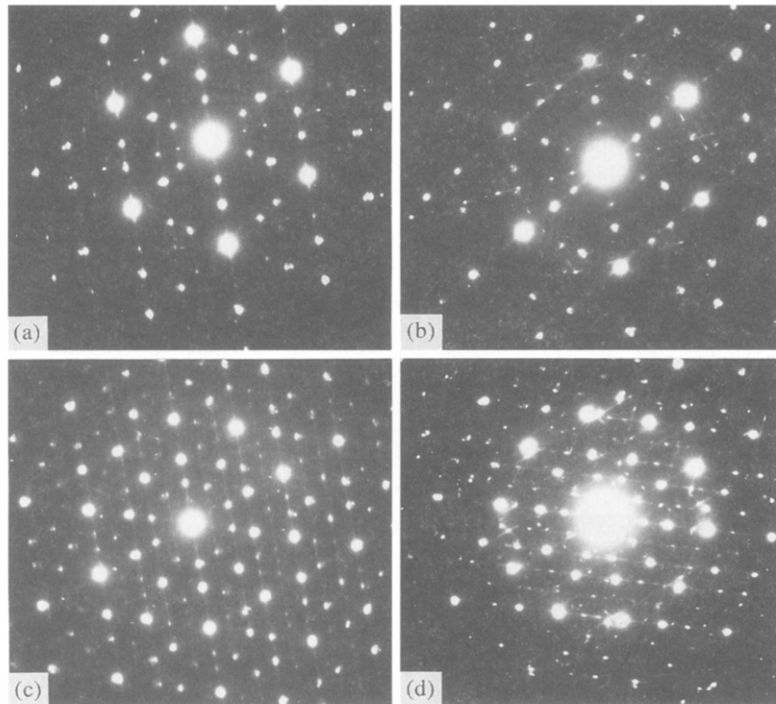


Fig. 4. (a) and (b) Diffraction patterns from two of the three orientations of pseudo parallel three-fold I zone axes from different grains in a cluster of decagonal phase grains in melt spun $\text{Al}_{12}\text{Mn}_{2.9}\text{Zn}$ alloy. (c) and (d) two of the five variants of the pseudo five-fold J zone axis orientation parallel to a ten-fold axis in the aggregate of decagonal grains.

4. DISCUSSION

4.1. Formation of quasicrystalline phases

The composition of the quasicrystalline phases in the Al–Mn alloys has been found to correspond to Al_4Mn [35]. Due to an increase in solubility on rapid solidification, the composition of the quasicrystals may show some variation. Although a combination of composition and cooling rate decides between the relative occurrence of icosahedral and the decagonal phases, a rigid criterion has not been evolved yet. It appears that the role of composition in deciding between the icosahedral and the decagonal phase may be limited to fixing the position of the liquidus which would then decide the level of undercooling if the temperature of the liquid is assumed to be constant. A similar argument has been advanced by Maamar *et al.* [18] to explain the formation of icosahedral and decagonal phases in Al–Mn–Cu alloys.

One thing very clearly established from this work is that the quasicrystal is readily formed in the composition corresponding to the T1 phase $\text{Al}_{24}\text{Mn}_5\text{Zn}$, which has an e/a ratio of 1.85 [7]. Robinson [7] has placed the T1 phase in the class of $\text{Al}_{60}\text{Mn}_{11}\text{Ni}_4$ and $\text{Al}_{20}\text{Mn}_3\text{Cu}_2$ due to its electronic structure, although its unit cell structure is very different from those of the latter two. Though a similarity to the lattice size would place T3 in the class of the $\text{Al}_{60}\text{Mn}_{11}\text{Ni}_4$ and $\text{Al}_{20}\text{Mn}_3\text{Cu}_2$, its stoichiometry is very different, $\text{Al}_{11}\text{Mn}_{2.8}\text{Zn}_{2.2}$, approximately $\text{Al}_2(\text{Mn},\text{Zn})$. The $\text{Al}_{60}\text{Mn}_{11}\text{Ni}_4$,

$\text{Al}_{20}\text{Mn}_3\text{Ni}_2$ and T1 phases are close to the stoichiometry Al_4Mn .

4.2. Epitaxial growth of the decagonal quasicrystal on icosahedral quasicrystal

The decagonal phase can grow epitaxially on the icosahedral seed. Bendersky [36] determined that the decagonal phase grows with its ten-fold axis along one of the five-fold axes of the icosahedral phase. Thus there are six possible variants of the decagonal phase nucleated on an icosahedral seed. Ranganathan and Chattopadhyay [37] pointed out that the aggregate of decagonal phase grains growing from the same seed will preserve the icosahedral symmetry. Lalla *et al.* [38] showed this orientation relationship to exist in an Al–Mn–Ge alloy. A similar relationship was observed by Lalla *et al.* [39] in Al–Mn–Ni alloys and it was pointed out that the pseudo five-fold axes of the decagonal phase will be parallel to one of the five-fold axes of the icosahedral phase and the pseudo three-fold axes will be parallel to one of the three-fold axes in the icosahedral phase. A similar relationship has been obtained in the case of the Al–Mn–Zn in the present study. Along the ten-fold axis of a decagonal phase variant in the aggregate (Fig. 4(c), (d)), the other five variants have one of their pseudo five-fold axes. Along a pseudo three-fold direction (Fig. 4(a), (b)) three variants of the pseudo three-fold I axis were observed. The other three variants are expected

to be pseudo three-fold M zone axes. Along the two-fold zone axis G two variants were observed (Fig. 3). The other four variants in the aggregate are expected to have one of their zone axes related to the icosahedral phase in this orientation. The composite diffraction pattern of two variants of the two-fold G zone axis (Fig. 3(c)) resembles a two-fold diffraction pattern of the icosahedral phase. Tiwari *et al.* [40] have considered this to be a twin of the decagonal phase. A twinning of the decagonal phase can thus be seen to be generating the icosahedral symmetry.

4.3. The crystalline phase

Robinson [7] has pointed out that in T1-AlMnZn phase the reflections with l odd are weak so that the

cell can be mistaken for a body centered one with half the a and c parameters. These weak reflections were not noticed in our diffraction patterns so the L phase could not be identified with T1, even though the composition of one of the alloys studied here corresponds to T1.

There have been two reports of the crystalline phases similar to those obtained here, with slightly different lattice parameters. A metastable phase has been reported in Al-Mn-Cr-Si alloys by Andersen *et al.* [41] and Guo *et al.* [42] with orthorhombic lattice parameters $a = 1.76$ nm, $b = 1.78$ nm and $c = 3.04$ nm. The diffraction patterns resemble those obtained from the L and M phases in this study. This phase occurred in the form of plates with stacking

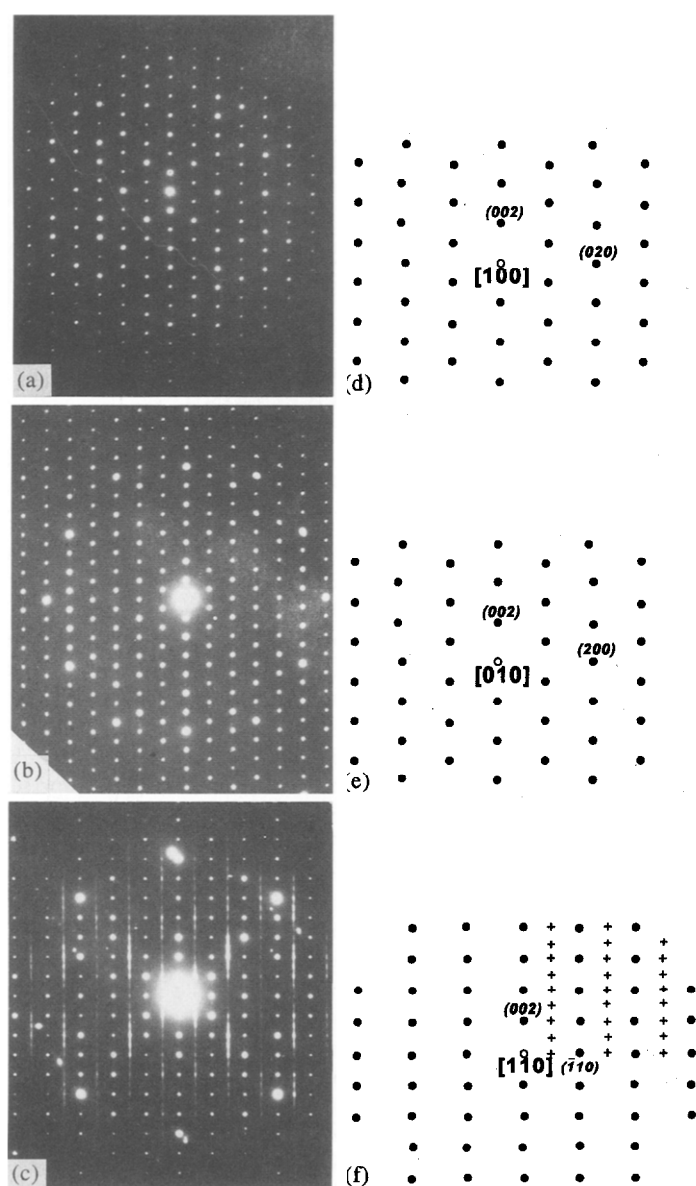


Fig. 5. The (a) [100], (b) [010] and (c) [110] zone axis patterns from the orthorhombic L phase obtained from the $\text{Al}_{12}\text{Mn}_{23}\text{Zn}$ alloy. (d), (e) and (f) are the schematics of these respective zone axes.

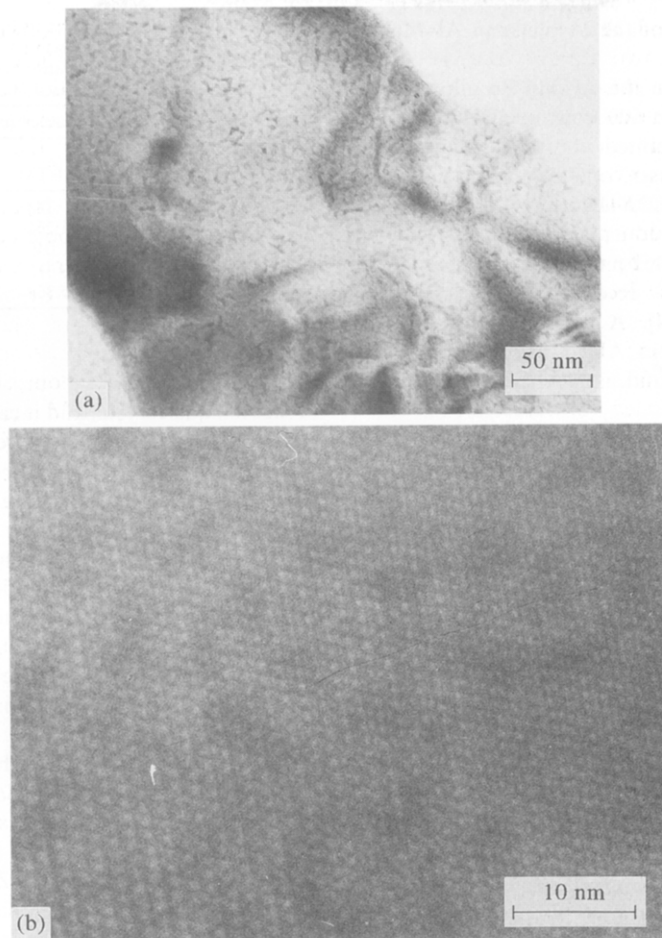


Fig. 6. (a) A low magnification micrograph of a L phase grain in [010] orientation in the melt spun $\text{Al}_{24}\text{Mn}_5\text{Zn}$ alloy aged at 600°C for 4 h. (b) A corresponding high resolution micrograph showing continuous fringes of same spacings but different contrast in L and M phases.

faults inside these plates. Twinning of this phase with 90° rotation around the c axis has been observed. The discontinuity in streaks in the [010] diffraction pattern is suggested to be due to the size effect of the twins.

Bendersky *et al.* [32] studied η $\text{Al}_{11}\text{Cr}_2$ phase and determined its lattice parameters to be monoclinic with $a = 1.76$ nm, $b = 3.05$ nm, $c = 1.76$ nm and $\beta \approx 90^\circ$, and possible space group as $C2/c$. These lattice parameters are close to those deduced for the M phase here. The single crystals of the η phase studied by Bendersky *et al.* [32] were usually found to be twinned, the twins being related by 90° around the b axis. The precession camera X-ray diffraction of these crystals suggested the lattice parameters to be body centered orthorhombic $a = 1.24$ nm, $b = 1.26$ nm and $c = 3.05$ nm, the same as the L phase studied here. Bendersky *et al.* [32] suggest that the η when solidified, a high-temperature less ordered orthorhombic phase formed first, which then transformed to a more ordered C-centered monoclinic phase low temperature phase. The two twin variants of the monoclinic phase arise due to the

pseudo tetragonality ($a \approx b$) of the orthorhombic phase.

After annealing the quasicrystals for one hour at 600°C , the M phase reciprocal spots are streaked and the bright field micrographs show an uneven distribution of this phase in L, while after annealing for four hours the reciprocal spots of M begin to get defined and there is an even distribution of this phase (Fig. 6(a)). Thus it appears that the quasicrystalline phases transformed to the L phase which then nucleated the M phase.

It is important to note here that the Al–Mn–Ni decagonal phase is also found to first transform to the L phase. This L phase then orders to produce an ordered phase other than the M phase [13]. This phase appears to be the same as a monoclinic one reported in an Al–Cr–Fe alloy with lattice parameters $a = 3.31$, $b = 1.23$, $c = 2.48$ nm and $\beta = 112^\circ$ [43]. That the quasicrystalline phases first transform to the L phase implies that this phase may be closest to the structure of the quasicrystals. Planar defects are observed in the L phase in Al–Mn–Ni alloy too [13]. These defects disappear on further transformation to

form the appearance of the M phase in Al–Mn–Zn alloys.

The final product in the $\text{Al}_{24}\text{Mn}_5\text{Zn}$ alloy after a prolonged annealing at 600°C is the λ - Al_4Mn phase. Murray *et al.* [33] pointed out that there are two Al_4Mn hexagonal phases, one is denoted as λ with lattice parameters $a = 2.841$ and $c = 1.238$ nm, and the another one denoted as μ has lattice parameters $a = 1.995$ and $c = 2.452$ nm. The structure of the μ - Al_4Mn phase has recently been solved by Shoemaker *et al.* [44]. A phase isomorphous to μ - Al_4Mn is reported in Al–Cr as the ϵ phase by Bendersky *et al.* [32] and as μ - Al_4Cr by Wen *et al.* [45].

Evidently, the transformation of the quasicrystalline phases to crystalline phases involves rearrangement of atoms. Due to this, the first crystalline product consists of periodic defects. On further ordering of atoms these defects disappear and another phase emerges. Thus a series of metastable structures emerge to finally arrive at the stable phase.

4.4. Approximants to the icosahedral and the decagonal quasicrystals

It was mentioned in Section 1 that the crystalline approximants can approximate the icosahedral or the decagonal phase. The crystalline approximants to the quasicrystalline phases can be of the type mimicking

Table 1. Lattice parameters for various orders of rational approximants to the icosahedral phase for Al–TM (TM = transition metal) and magnesium based alloy [46]

Approximant	Lattice parameter (nm)	
	Al–TM	Mg based
q/p		
1/0	0.783	0.847
1/1	1.266	1.431
2/1	2.049	2.136
3/2	3.315	3.747
5/3	5.364	6.037

the icosahedral phase or the two-dimensional decagonal quasicrystal and it can be shown that these two kinds of approximants are distinct [46].

The major axes a , b and c of an orthorhombic approximant to the icosahedral phase are related to three mutually perpendicular two-fold axes of the icosahedral quasicrystal. Each of the three lattice parameters of the orthorhombic approximant can be approximated as q/p so that the approximant can be represented as $[(q_1/p_1), (q_2/p_2), (q_3/p_3)]$. The correspondence between the lattice parameters and q/p value is shown in Table 1. An example of a $(\frac{3}{2}, \frac{2}{1}, \frac{1}{1})$ orthorhombic approximant is in a Mg-based alloy [24]. In the case of the orthorhombic decagonal approximants usually the b lattice parameter corresponds to the decagonal axis while the other two parameters correspond to the two two-fold axes of the decagonal phase. Thus, Zhang and Kuo [47] proposed that the decagonal approximants be represented as $[(q_1/p_1), (q_2/p_2)]$, the q/p values corresponding to the a and c axes. The values of a and c corresponding to q/p values are approximately those shown in columns two and three in Table 1.

The L phase has recently been reported in $\text{Al}_{12}\text{Fe}_2\text{Cr}$ alloy where it has been considered as an approximant to the decagonal quasicrystal [43]. The [010] zone axis pattern (see Fig. 5(b)) resembles a pseudo ten-fold due to a ring of intense spots. Further, the b parameter of about 1.26 nm is equal to the periodicity along the decagonal axis in the same alloy. The a parameter of the L phase would thus be a 1/1 approximant (refer to column 2 of Table 1). However, the c parameter does not correspond to any value in column 3 of Table 1 for the determination of q/p value. Sui *et al.* [43] thus called this phase a “non-Fibonacci” approximant.

Instead, let us consider the L phase to be an approximant to the icosahedral quasicrystal. The a and b parameters then correspond to 1/1 approximation. If 1.24 nm is approximated by 1/1, then $1.24\tau^2 = 3.246$ nm is approximated by 3/2. The reported c parameters of the L phase in various alloys range between 3.02 to 3.14 nm. Thus the c parameter is close to 3/2 approximation and the L phase is a (1/1–1/1–3/2) approximant.

The interpretation of the diffracted intensities of the L phase obtained in a Al–Mn–Ni alloy [13] has been done elsewhere [46]. In the orthorhombic

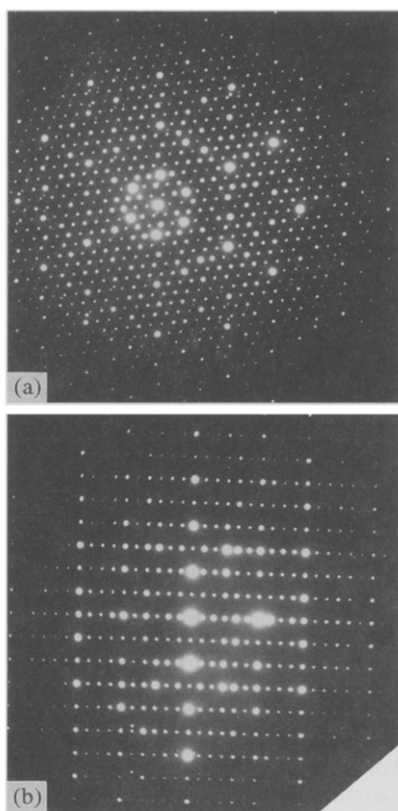


Fig. 7. (a) [001] and (b) [100] zone axis electron diffraction patterns from the hexagonal λ - Al_4Mn type phase in the melt-spun $\text{Al}_{24}\text{Mn}_5\text{Zn}$ alloy aged at 600°C for 25.5 h.

Table 2. A list of quasicrystalline phases and their crystalline approximants in Al–Mn–Ni, Al–Mn–Cu and Al–Mn–Zn alloys

System/Phase	Al–Mn–Ni	Al–Mn–Cu	Al–Mn–Zn
Icosahedral Quasicrystal	Al ₆₀ Mn ₁₁ Ni ₄ [39] Al ₈₀ Mn ₁₃ Ni ₇ [39]	Al ₇₆ Mn _{15.5} Cu _{8.5} [14] Al _{74.5} Mn _{12.5} Cu ₁₀ [16] Al ₇₉ Mn ₁₃ Cu ₈ [16] Al ₅₇ Mn _{32.5} Cu _{10.5} [17] Al ₆₅ Mn ₂₀ Cu ₁₅ [17]	Al ₂₄ Mn ₅ Zn [13], present study
Decagonal Quasicrystal	Al ₆₀ Mn ₁₁ Ni ₄ [12, 13, 39] Al ₈₀ Mn ₁₃ Ni ₇ [39]	Al ₇₉ Mn ₁₃ Cu ₈ [16] Al ₁₀ Mn ₃ Cu _{0.1-0.2} [15] Al ₇₅ Mn ₁₀ Cu ₁₅ [17] Al ₅₇ Mn _{32.5} Cu _{10.5} [17] Al ₆₅ Mn ₂₀ Cu ₁₅ [17]	Al ₁₂ Mn _{2.9} Zn [13], present study
Taylor Approximate	—	Al ₇₆ Mn _{15.5} Cu _{8.5} [13, 14] Al ₆₀ Mn ₂₀ Cu ₁₅ [13] Al ₁₀ Mn ₃ Cu _{0.1-0.2} [15]	—
Robinson approximate	Al ₆₀ Mn ₁₁ Ni ₄ [12]	Al ₇₆ Mn _{15.5} Cu _{8.5} [13, 14] Al ₆₀ Mn ₂₀ Cu ₁₅ [13] Al ₁₀ Mn ₃ Cu _{0.1-0.2} [15] Al ₇₅ Mn ₁₀ Cu ₁₅ [17, 18] Al ₆₅ Mn ₂₀ Cu ₁₅ [17, 18]	—
Little Approximant	Al ₆₀ Mn ₁₁ Ni ₁₄ [13]	—	Al ₂₄ Mn ₅ Zn Al ₁₂ Mn _{2.9} Zn [13], present study
Monoclinic M Approximant	—	—	Al ₂₄ Mn ₅ Zn Al ₁₂ Mn _{2.9} Zn [13], present study

approximants to the icosahedral phase the major axes $\langle 100 \rangle$ correspond to three of the two-fold axes of the icosahedral phase. Thus in the diffraction patterns of Fig. 5 the strong spots $\{0\ 13\ 3\}$ in zone axes $[100]$ and $[010]$ correspond to the vertex vector spots along the five-fold axes of an icosahedral phase.

The orthorhombic approximants to the decagonal quasicrystal can transform to monoclinic approximants, some of which are listed by Henley [48]. These monoclinic approximants are characterized by a β parameter close to 72° or 108° and multiply twin to generate a ten-fold symmetry. Since the L phase is an orthorhombic approximant to the icosahedral phase it transforms to a monoclinic phase M with $\beta \approx 90^\circ$ (and not 72° or 108°) in Al–Cr [32], Al–Mn–Cr–Si [41, 42] and Al–Mn–Zn.

4.5. A comparative study

Table 2 summarises the approximant structures found in Al–Mn–Ni, Al–Mn–Cu and Al–Mn–Zn systems. There is no report of a single icosahedral phase in an Al–Mn–Ni alloy while there are several for a single decagonal phase. Thus it can be concluded that the decagonal phase formation is preferred in the Al–Mn–Ni alloys. The Al–Mn–Cu and the Al–Mn–Zn alloys appear to show an equal preference for icosahedral and decagonal phases. The Al–Mn–Cu alloys form the Taylor and Robinson approximants to the decagonal phase. The Al–Mn–Ni decagonal phase has been shown to transform to a Robinson related phase at 400°C by Van Tendeloo *et al.* [12]. Singh and Ranganathan [13] found this decagonal phase to transform to the Little approximant at a higher temperature. In the present study on Al–Mn–Zn the icosahedral phase has been observed to transform to the L and M approximants to the icosahedral phase. At the same time, the decagonal

phase in this system also transforms to the L and M phases.

Although the T3–AlMnZn phase is isostructural to the Al₂₀Mn₃Cu₂ and Al₆₀Mn₁₁Ni₄, considered good candidates for the decagonal phase, this work has not been able to establish a direct relationship between T3 and the decagonal phase. In the Al₆₀Mn₁₁Ni₄ [12] too the decagonal phase transformed to two phases at 400°C . In the Al–Mn–Cu alloy decagonal phase approximants are well known Al₃Mn and Al₂₀Mn₃Cu₂ phases [14, 15].

5. CONCLUSIONS

After a study of two Al–Mn–Zn alloys of composition Al₂₄Mn₅Zn (corresponding to the T1 ternary phase) and Al₁₂Mn_{2.9}Zn in melt-spun condition, the following conclusions are made

1. Melt spinning leads to the formation of the icosahedral phase in Al₂₄Mn₅Zn alloy and the decagonal phase in the Al₁₂Mn_{2.9}Zn alloy.
2. The decagonal phase grains in the Al₁₂Mn_{2.9}Zn alloy occurred in aggregates containing six orientational variants related by an icosahedral symmetry.
3. Both the quasicrystals transformed on annealing at 500 and 600°C to an orthorhombic phase L (body centered, $a = 1.24$, $b = 1.26$ and $c = 3.05$ nm), which then transforms to a more ordered C-centered monoclinic phase M with lattice parameters $a = c = 1.77$, $b = 3.05$ nm and $\beta = 89.1^\circ$.
4. The M phase is not well formed till one hour of annealing at 600°C and its reciprocal points are streaked. However, after a four hour anneal the reciprocal spots become more defined and the

distribution of the phase in the L phase very uniform.

5. The L phase is shown to be an approximant to the icosahedral quasicrystal.
6. A prolonged annealing of 25.5 h at 600°C gives rise to a λ -Al₄Mn type hexagonal phase with lattice parameters $a = 2.85$ and $c = 1.24$ nm in Al₂₄Mn₅Zn.

Acknowledgements—The authors are grateful to Professor K. Chattopadhyay, Dr B. B. Rath, Dr C. S. Pande, Professor S. Mahajan and Dr U. Dahmen for stimulating discussions. Financial support from the Office of the Naval Research, U.S.A., under the Indo-U.S. Cooperation project entitled "Quasicrystals and Crystalline Interfaces" (ONR grant N 00014-95-1-0095) is gratefully acknowledged.

REFERENCES

1. Shechtman, D., Blech, I., Gratias, D. and Cahn, J. W., *Phys. Rev. Lett.*, 1984, **53**, 1951.
2. Chattopadhyay, K., Lele, S., Ranganathan, S., Subbanna, G. N. and Thangaraj, N., *Current Science*, 1985, **54**, 895.
3. Bendersky, L., *Phys. Rev. Lett.*, 1985, **55**, 1461.
4. Elser, V. and Henley, C. L., *Phys. Rev. Lett.*, 1985, **55**, 2883.
5. Ishihara, K. N., *Mater. Sci. Forum*, 1986, **22–24**, 223.
6. Raynor, G. V. and Wakeman, D. W., *Proc. Roy. Soc. A*, 1947, **190**, 83.
7. Robinson, K., *Phil. Mag.*, 1952, **43**, 775.
8. Damjanovic, A., *Acta Cryst.*, 1961, **14**, 982.
9. Robinson, K., *Acta Cryst.*, 1954 **7**, 494.
10. Ranganathan, S. and Chattopadhyay, K., *Phase Transitions*, 1989, **16/17**, 67.
11. Audier, M., Duneau, M. and Vacher, M., *Proc. Intl. Conf. Advances in Physical Metallurgy*, ed. S. Banerjee. Bombay, 1994.
12. Van Tendeloo, G., Van Laduyt, T., Amelinckx, S. and Ranganathan, S., *J. Microsc.*, 1988, **149**, 1.
13. Singh, Alok and Ranganathan, S., *Mater. Sci. Eng.*, 1994, **A181/A182**, 754.
14. Van Tendeloo, G., Singh, Alok and Ranganathan, S., *Phil. Mag. A*, 1991, **64**, 413.
15. Li, X. Z. and Kuo, K. H., *Phil. Mag. B*, 1992, **66**, 117.
16. Ebalard, S. and Spaepen, F., *J. Mater. Res.*, 1990, **5**, 62.
17. Maamar, S. and Harmelin, M., *Philos. Mag. Lett.*, 1991, **64**, 343.
18. Maamar, S., Faudot, F. and Harmelin, M., *Thermochim. Acta*, 1992, **204**, 45.
19. Schaefer, R. J. and Bendersky, L., *Scripta Metall.*, 1986, **20**, 745.
20. Lilienfeld, D. A., Hung, L. S. and Mayer, J. W., *MRS Bulletin*, 1987, Feb–March, 31.
21. Cooper, M. and Robinson, K., *Acta Cryst.*, 1966, **20**, 614.
22. Bergman, G., Waugh, J. L. and Pauling, L., *Acta Cryst.*, 1957, **10**, 254.
23. Spaepen, F., Chen, L. C., Ebalard, S. and Ohashi, W., in *Quasicrystals*, ed. M. V. Jaric and S. Lundqvist. World Scientific, Singapore, 1990, p. 1.
24. Edagawa, K., Suzuki, K., Ichihara, M., Takeuchi, S., Kamiya, A. and Mizutani, U., *Philos. Mag. Lett.*, 1991, **64**, 95.
25. Taylor, M. A., *Acta Metall.*, 1960, **8**, 256.
26. Fitz Gerald, J. D., Withers, R. L., Stewart, A. M. and Calca, A., *Phil. Mag. B*, 1988, **58**, 15.
27. Daulton, T. L., Gibbon, P. C. and Kelton, K. F., 1991, **63**, 687.
28. Li, X. Z. and Kuo, K. H., *Philos. Mag. B*, 1992, **65**, 525.
29. Thangaraj, N., Subbanna, G. N., Ranganathan, S. and Chattopadhyay, K., *J. Microsc.*, 1987, **146**, 287.
30. Ranganathan, S., Singh, Alok, Mukhopadhyay, N. K. and Weatherly, G. C., *Scripta Metall. Mater.*, 1994, **30**, 271.
31. Little, K., Dissertation, University of Oxford, UK, 1949, cited in reference [7].
32. Bendersky, L. A., Roth, R. S., Ramon, J. T. and Shechtman, D., *Metall. Trans. A*, 1991, **22A**, 5.
33. Murray, J. L., McAlister, A. J., Schaefer, R. J., Bendersky, L. A., Biancaniello, F. S. and Moffat, D. L., *Metall. Trans. A*, 1987, **18A**, 385.
34. Bendersky, L. A., *Materials Science Forum*, 1987, **22–24**, 151.
35. Inoue, A., Arnberg, L., Lehtinen, B., Oguchi, M. and Masumoto, T., *Metall. Trans.*, 1986, **17A**, 1657.
36. Bendersky, L. A., *J. Physique*, 1986, **47**, C3-457.
37. Ranganathan, S. and Chattopadhyay, K., *Key Engg. Mater.*, 1987, **13–15**, 229.
38. Lalla, N. P., Tiwari, R. S. and Srivastava, O. N., *J. Mater. Res.*, 1992, **7**, 1.
39. Lalla, N. P., Tiwari, R. S. and Srivastava, O. N., *Philos. Mag. B*, 1991, **63**, 629.
40. Tiwari, R. S., Lalla, N. P. and Srivastava, O. N., *J. Non-Cryst. Solids*, 1993, **153 & 154**, 508.
41. Anderson, S. J., Guo, Y. X., Nylund, H. K. and Hoier, R., *Electron Microscopy*, Vol. 2, EUREM 92. Granada, Spain, 1992, p. 219.
42. Guo, Y. X., Andersen, S. J., Nylund, H. K. and Hoier, R., *Micron and Microscopia Acta*, 1992, **23**, 165.
43. Sui, H. X., Liao, X. Z. and Kuo, K. H., *Phil. Mag. Lett.*, 1995, **71**, 139.
44. Shoemaker, C. B., Keszler, D. A. and Shoemaker, D. P., *Acta Cryst.*, 1989, **B45**, 13.
45. Wen, K. Y., Chen, Y. L. and Kuo, K. H., *Metall. Trans.*, 1992, **23A**, 2437.
46. Singh, Alok, Ramakrishnan, K. and Ranganathan, S., *Phil. Mag.* (submitted for publication).
47. Zhang, Z. and Kuo, K. H., *Phys. Rev.*, 1990, **B42**, 8907.
48. Henley, C. L., *J. Non-Cryst. Solids*, 1985, **75**, 91.